Sci. Rep., Niigata Univ. (Geology), No. 19, 1-13, 2004

Quantitative analysis of rock-forming minerals using the energy-dispersive X-ray spectrometer

Hiroshi KAWABATA*, Toshiaki SHIMURA** and Makoto SATO***

Abstract

This paper describes the sources of error and the methods for quantitative analysis using an energy-dispersive X-ray spectrometer. On the probe current correction method used in this system, the accuracy is significantly affected by the intensity of the cobalt $K\alpha$ line. A 1% difference in cobalt intensity or probe current shifts the oxide concentration by about 1%. Therefore, calibration using the appropriate X-ray intensity of cobalt and a steady probe current are essential in obtaining satisfactory results. Another potential error source is distortion of the spectrum caused by characteristics of the semiconductor detector. Although the sum peak and escape peak can be avoided by careful identification of the peaks, silicon internal fluorescence X-ray is not distinguishable from the original Si $K\alpha$ emanating from the sample, and causes an overestimation of about 0.15% Si. Since incomplete charge collection also overestimates concentration, especially for low energy elements, correction for incomplete charge collection is required to analyze low energy trace elements accurately. Analytical results of minerals and a glass indicate that oxides with concentrations >0.7% can be analyzed with a less than 10% RSD (relative standard deviation), and are in agreement with the results using the wavelength-dispersive X-ray spectrometer.

Key words: EDS, energy-dispersive X-ray spectrometer, EPMA, Oxford Link ISIS.

Introduction

EPMA (electron probe microanalyzer) is divided into two methods based on the X-ray spectrometry: WDS (wavelength dispersive X-ray spectrometry) and EDS (energy-dispersive X-ray spectrometry). Since each detector type has its advantages and disadvantages, it is desirable

---

* Institute for Frontier Research on Earth Evolution (IFREE), Japan Marine Science and Technology Center (JAMSTEC), Yokosuka 237-0061, Japan

** Department of Geology, Faculty of Science, Niigata University, Niigata 950-2181, Japan

*** Graduate School of Science and Technology, Niigata University, Niigata 950-2181, Japan

(Manuscript received 18 August, 2003 accepted 10 December, 2003)

to use the one most suited for each purpose.

When electrons impact the atoms in samples, X-rays that have various energies /wavelengths are generated. In WDS, only X-rays with a certain wavelength diffracted by a diffracting crystal enter the detector. Use of a diffracting crystal improves the detection limit due to the high contrast between peak and background intensity, but also requires a relatively high probe current as X-ray sensitivity is reduced. In EDS, on the other hand, X-rays with various energies that enter the detector are accumulated by a multi-channel analyzer for whole energy to produce a spectrum. Because EDS is not equipped with diffracting crystals, spectral resolution and peak/background ratio is inferior to WDS, which results in spectral overlapping and insensitivity of detection. However, the nature of the EDS permits us to measure multiple elements simultaneously under the relatively low probe currents. Thus, EDS is not suited for the measurement of trace elements, but is suited for the analysis of samples which are easily damaged by probe currents (glass, carbon silicate, etc).

Collection of X-rays from a relatively large area is also better suited to EDS. Since WDS needs to satisfy Bragg's condition of diffraction, collection of X-rays from a relatively large area diminishes X-ray intensity at the margin of analytical area. Thus, EDS is a more effective method for obtaining the bulk composition of reaction products or the groundmass of volcanic rocks, for example.

In this paper, we present quantitative analytical methods for mineral and glass using an energy-dispersive X-ray spectrometer, and discuss the factors controlling the accuracy and precision of the analysis.

Equipment and analysis procedure

Chemical analyses were made using a scanning electron microscope (JEOL JSM-5600) equipped with energy dispersive X-ray spectrometer (Oxford Link ISIS-310) at Niigata University. A Si (Li) detector with a SATW window was installed at 33° take-off angle. The detector was kept cool using liquid nitrogen, to suppress both the diffusion of Li and noise. The spectra are collected using a multi-channel analyzer with 1024 channels of 10 eV each. Resolution was 138 eV at 5.9 keV on the Mn $K\alpha$ peak. Analyses were performed with an accelerating voltage of 15 kV, probe current of 1.00 nA, and a counting time of 100 seconds at a working distance of 20 mm. The stability of the probe current affects the analytical accuracy. In this system, it takes about one hour to stabilize the probe current after heating the filament. We monitored current drift before and after each analysis, and rejected the data obtained when the drift was greater than 0.5%.

The quantitative analytical procedure is shown in Fig. 1. Before analyzing unknown sample, it is necessary to analyze a cobalt standard and calibrate the EDS using cobalt spectrum. The cobalt spectrum is used for the probe current correction, resolution measurement, and gain calibration. Next, we register a profile, which is the spectrum within a region of interest

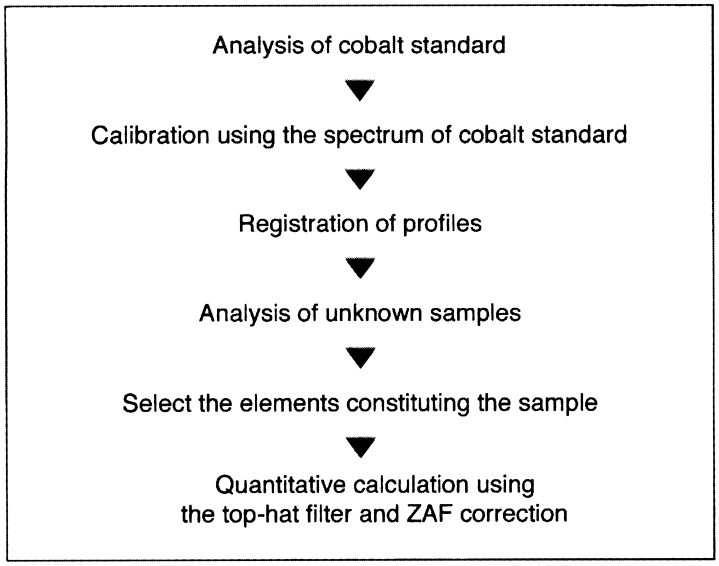

Fig. 1. Procedure for quantitative analysis using the energy-dispersive X-ray spectrometer.

(ROI), using standard materials for each element. The details of registration will be described in the next section. Re-registration of the profiles is not required unless the system conditions change. System stability for EDS is better than for WDS, as the former has few movable devices. Therefore, we can skip the registration step in routine usage. After calibration and registration, we collect X-rays from unknown samples and identify peaks on the spectrum. The elements comprising the sample are thus identified for quantitative calculation using the Oxford-supplied software.

The software installed to the Oxford Link ISIS-310 EDS system performs the following processing. First, spectrum profiles of unknown sample is converted by mathematical filtering known as top-hat filtering. For EDS, the background is subtracted by this filtering, whereas for WDS, it is subtracted by using the X-ray intensity on both sides of the tails of a characteristic peak. Second, the converted standard spectrum profile is scaled to match the converted spectrum of unknown sample. The net intensity used for the *ZAF* correction (e.g., Statham, 1979; Kinouchi, 2001) is the overlapping region of the converted spectra between the sample and standard profiles (c.f. Fujino and Itaya, 1992). Like this way, EDS uses the integrated counts within the ROI set around the peak centroid, rather than the intensity of the peak centroid, to determine the intensity of the characteristic X-ray. This is because of the poor resolution of the spectrometer (Goldstein et al., 2003). Finally, the *ZAF* correction is carried out using the relative intensity of the standard profiles and the unknown sample (*K*-ratio).

Table 1. Standard materials used for the registration of profiles and the ratio factor correction.

	Profile			Ratio factor correction
Element	Standard material	ROI (keV)	X-ray line	mineral
Si	SiO_2	1.739−1.840	$K\alpha$	−
Ti	TiO_2	4.505−4.965	$K\alpha$	Pyroxene
Al	Al_2O_3	1.486−1.560	$K\alpha$	Sillimanite
Cr	Cr_2O_3	5.406−5.989	$K\alpha$	−
Fe	Fe_2O_3	6.391−7.111	$K\alpha$	Olivine
Mn	$MnO\text{-}Fe_2O_3$	5.888−6.538	$K\alpha$	Rhodonite
Mg	MgO	1.254−1.303	$K\alpha$	Olivine
Ca	$CaSiO_3$	3.688−4.038	$K\alpha$	Wollastonite
Na	NaCl	1.041−1.072	$K\alpha$	Jadeite
K	$KTiOPO_4$	3.311−3.608	$K\alpha$	Adularia
Ni	NiO	7.461−8.332	$K\alpha$	−

(ROI, region of interest.)

Standard materials

Table 1 lists standard materials used for the registration of profiles and for the correction of ratio factor. We selected oxides and a chloride that have no overlapping characteristic X-ray peaks. To correct the profile intensity, the ratio factor correction proposed by Yokoyama et al. (1993) was applied using stoichiometry and reference values of silicate minerals.

Result and discussion

To obtain accurate results, it is necessary to consider the sources of errors and their effects on the results. We shall focus on the influence of probe current correction, the distortion of spectrum resulting from characteristics of Si (Li) detector, and alkali loss.

1. Correction for probe current

The basis of quantitative analysis by EPMA is to compare characteristic X-ray intensities between a standard and the unknown sample. The ratio of X-ray intensity in the sample to that in the standard is approximately equivalent to the ratio of concentration in the sample to that in the standard. Since the X-ray intensity is proportional to the probe current (Fig. 2), the correction for fluctuations in the probe current is essential. In our procedure, the correction for probe current is performed not by actual current value, but by cobalt standard intensity. In other

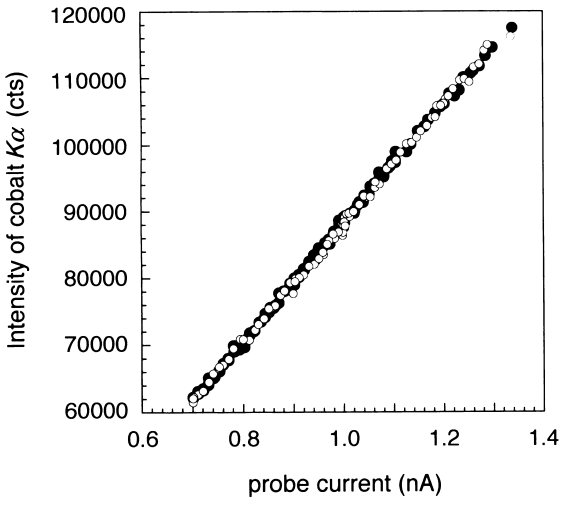

Fig. 2. Electron probe current versus intensity of cobalt $K\alpha$ line. Open circles and solid circles represent the data obtained with a focused beam and by area analysis, respectively. The relationship between the probe current and the intensity of cobalt is not dependent on analytical area.

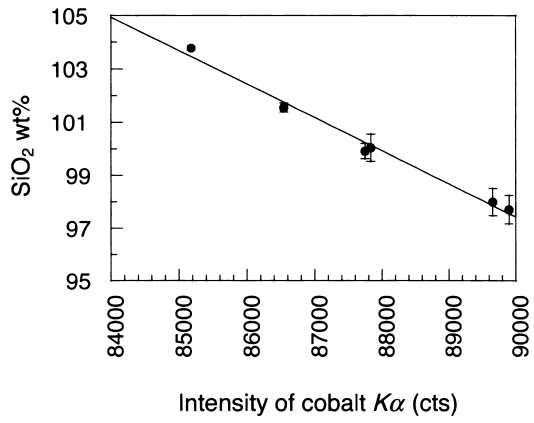

Fig. 3. Relationship between the calculated composition of quartz and the intensity of cobalt standard used for calibration. Error bars represent the standard deviation (1σ). Solid line represents the regression line calculated using a linear equation.

words, differences in cobalt intensity are regarded as differences in probe current. Specifically, when we analyze a sample, the most recent cobalt intensity used for the calibration prior to the analysis of unknown sample is automatically recorded in a file together with the spectrum of the sample. Probe current correction is performed by a direct comparison between the cobalt intensity saved with the standard profile and the cobalt intensity saved with the spectrum of the unknown sample.

Fig. 2 shows the relationship between probe current and the X-ray intensity of the cobalt $K\alpha$ line. If the probe current increases by 0.1 nA, cobalt intensity increases by 9000 cts (count total second). This relationship holds for analyses up to relatively large areas (at least < $4.5 \times 10^3 \mu m^2$)

In order to examine what extent the change in cobalt intensity influences the probe current

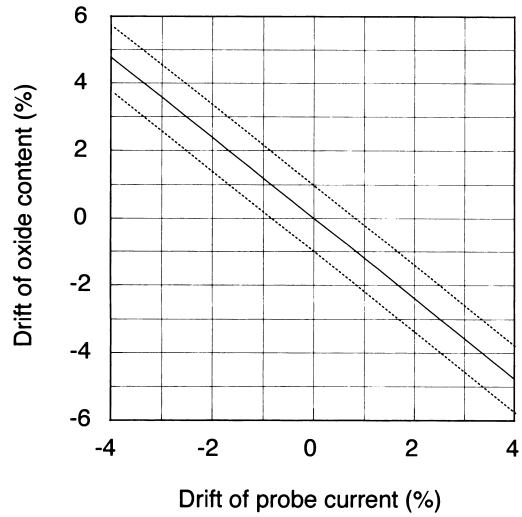

Fig. 4. Variation of the calculated oxide content resulting from drift of the probe current. Dashed lines represent the standard deviation of 1%.

correction, we analyzed quartz under the various calibration conditions. Although the quartz was analyzed at a probe current of 1.00 nA, a cobalt standard was analyzed under various probe currents to obtain a range in intensities. As shown in Fig. 3, the results of the quantitative calculation have a large variation depending on cobalt intensity. A 800 cts increase in the cobalt intensity used for the calibration reduces SiO_2 content by 1 wt%. Because the intensity of Si $K\alpha$ is nearly constant in this series of analyses, the variation in SiO_2 is explained by the amount of probe current correction.

The relationship among probe current, cobalt intensity, and calculated oxide content, obtained from Figs. 2 and 3, allows us to examine the effect of current drift on the precision of the analysis. A variation of approximately 1% in probe current (we permitted less than 0.5% variation in current drift during an acquisition) results in a variation of about 1.2% in SiO_2 content for the quartz (Fig. 4). Thus, in order to obtain accurate and precise results, it is necessary to use the appropriate cobalt intensity as the calibrated value, and to keep the probe current constant during analysis. Since this machine does not take account actual current drift, the appropriate cobalt intensity is an important point during analytical run.

2. Silicon internal fluorescence X-ray

X-rays which strike the silicon dead layer in the Si (Li) detector excite the silicon constituting the detector and generate Si internal fluorescence X-rays. The silicon internal fluorescence X-ray is not distinguishable from the original Si $K\alpha$ emanated from the target. The intensity of silicon internal fluorescence X-ray is mainly controlled by take-off angles, and differs from system to system. The reported values of silicon internal fluorescence X-ray observed in EDS range from 0.12% to 0.30% (Yokoyama et al., 1993; Goldstein et al., 2003). In 40 analyses of

metals, an average of 0.15% Si was detected with a standard deviation of 0.12%. Because the metals analyzed do not contain silicon, the detected Si is attributed to silicon internal fluorescence X-rays.

3. Sum peak and escape peak

Sum peaks appear when two photons enter a detector simultaneously and the pile-up rejection does not work. A sum peak has an energy equal to the sum of the two photons. Effect of sum peaks on the results can be avoided by not selecting that peak in the calculation procedure.

When silicon internal fluorescence is generated, incident X-rays lose the energy equivalent to the energy of Si $K\alpha$ (1.740 keV). This phenomenon produces an escape peak, which appears at an energy that is lower than the original energy by 1.740 keV. Escape peaks can be automatically removed by the Link ISIS software.

4. Incomplete charge collection

Incident X-rays produce electron-hole pairs in a Si (Li) detector. The number of pairs is proportional to the energy of the incident X-rays. Electrons generated near the faces and side of the detector tend to not be conducted toward the electrode. This phenomenon is known as 'incomplete charge collection', which lowers the energy of incident X-rays measured and causes an asymmetrical distortion of the low-energy side of the peak (Mori and Kanehira, 1984; Goldstein et al., 2003).

The extent of incomplete charge collection is a function of energy (Goldstein et al., 2003), and X-rays with low energy frequently cause incomplete charge collection. For example, in the analysis of a Mg-rich olivine, the low energy tail of the spectrum resulting from the incomplete charge collection of Mg $K\alpha$ (1.253 keV), causes an overestimation of the intensity of Na $K\alpha$ (1.041 keV). When we calculated the composition of olivine from the sample listed in Table 2, 0.14% Na_2O was detected. The effect of incomplete charge collection can be avoided by not selecting the element affected by incomplete charge collection in the calculation procedure. However, if the element affected by incomplete charge collection is a constituent of the sample, this method cannot be used. If you need an accurate analysis of the low energy elements, the correction procedure for incomplete charge collection described by Mori and Kanehira (1984) is required.

5. Alkali loss during analysis

Alkali loss has been reported particularly during the analysis of glasses and alkali-rich minerals (e.g., Nielsen and Sigurdsson, 1981; Gedeon et al., 2000). Alkali loss is believed to result from alkali ions being separated from the bridging oxygen and diffusing out of the excited volume (Lineweaver, 1962). This phenomenon also increases the concentration of elements (e.g., Si and Al) other than the alkalis (Devine et al., 1995).

Figure 5 shows results of analyses of a glass standard (NIST, SRM-616). The degree of Na

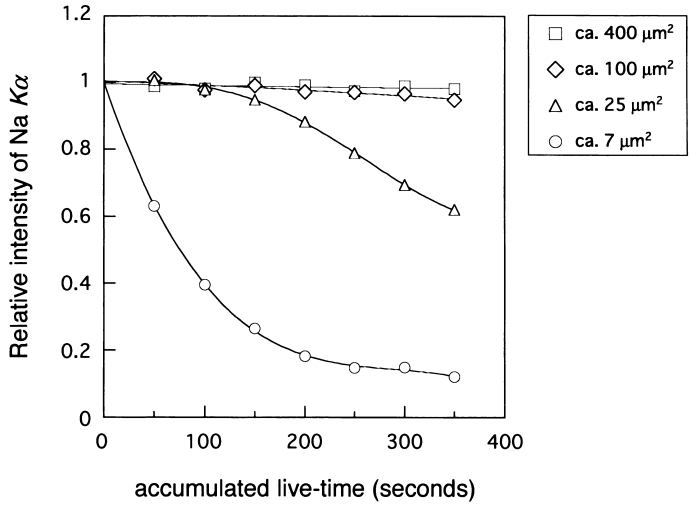

Fig. 5. Degree of Na loss during the analysis of a glass (NIST glass, 616). The extent of Na loss depends on the analytical duration and the analytical area. A decrease in Na is not observed for an analytical area of 400μm^2. Relative intensity was normalized using the maximum intensity of sodium obtained using an analytical area of 400μm^2 and based on the assumption that the maximum intensity represents the original Na intensity without Na loss. Regression curves were calculated using a polynomial equation.

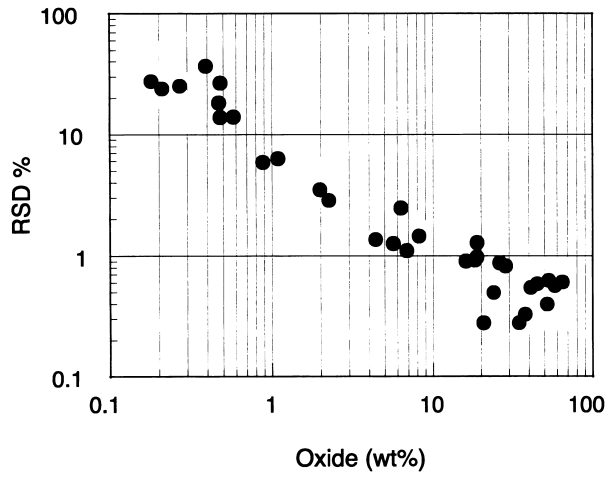

Fig. 6. Relative standard deviation (RSD) versus oxide content. The data used for this figure are obtained from the replicated analyses of minerals over 10 times (Table 2).

loss changes depending on the analytical duration and the analytical area. For the point analyses (analytical area ~7μm^2), the X-ray intensities decrease rapidly with time. The extent of Na loss is reduced with increasing analytical area, and the decrease in Na is not observed for an analytical area of 400μm^2. Thus, when we analyze a glass with a live-time of 100 seconds, Na loss can be ignored for areas larger than ~400μm^2 .

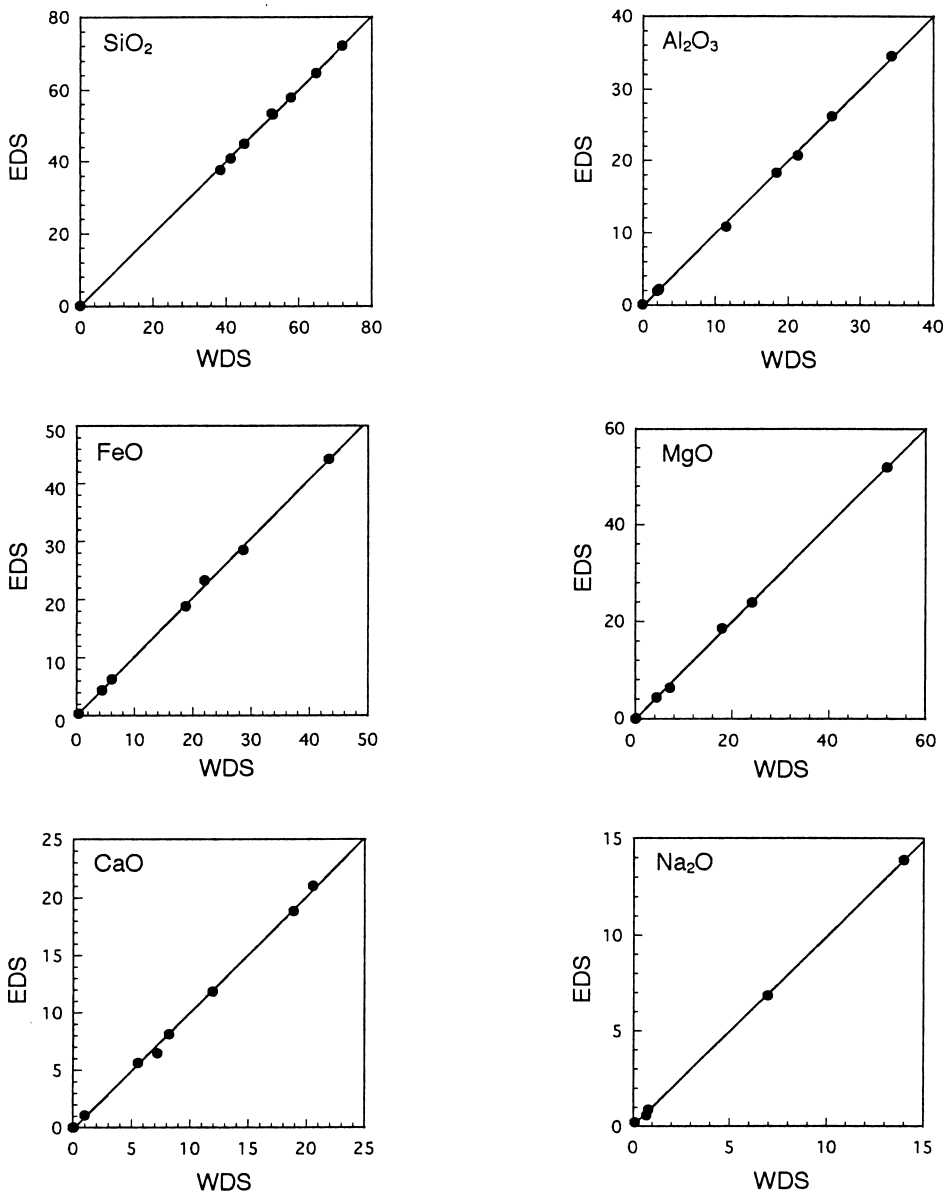

Fig. 7. Comparison of oxide content (wt%) determined with the energy-dispersive X-ray spectrometer versus wavelength-dispersive X-ray spectrometer. Solid lines represent the regression line calculated using the linear equation. The data used for this figure are obtained from the analytical results of minerals (Table 2).

6. Precision and accuracy

The analytical results of rock-forming minerals and a glass are given in Table 2, together with data obtained by WDS (JEOL JXA-8600) for comparison. Precision can be examined using the standard deviation, which includes the heterogeneity of samples. Standard deviation of the analytical totals is 0.27-0.63% (Table 2). Fig. 6 shows the relationship between relative standard deviation (RSD) and the oxide concentration. RSD increases exponentially with decreasing concentration, and will reach approximately 100% RSD at a concentration of 0.1 wt%. Since the detection limit for EDS is generally about 0.1 wt% (Reed and Ware, 1975; Goldstein et al., 2003), reproducibility for trace elements is poor. For the analysis of oxides of less than 0.7 wt%, it is necessary to change the analytical conditions. Alternatively, WDS may be used for precise analysis, as its detection limit is about 0.01 wt%. By contrast, for oxides comprising more than 0.7% of the sample, we can analyze with a precision of better than 10% RSD. Accuracy was examined using the mean analytical total and stoichiometry. The mean analytical totals fall within the range of 99 to 101 wt%, and the cation balance of minerals is consistent with stoichiometry. As shown in Fig. 7, the data obtained by EDS is in agreement with that by WDS. For other oxides, such as TiO_2, K_2O, Cr_2O_3, MnO, and NiO, agreement between EDS and WDS is acceptable (Table 2). The exception is the spinel and Fe-Ti oxide, for which overestimation of SiO_2 resulting from silicon internal fluorescence X-rays is significant because of the low concentration of SiO_2.

Conclusions

Rock-forming minerals and a glass were analyzed using the energy-dispersive X-ray spectrometer (Oxford Link ISIS-310) at Niigata University. In quantitative analysis, accurate correction for probe current requires a stable probe current and calibration using an appropriate cobalt intensity. For that, monitoring the secular variations of detector condition and cobalt standard intensity is important. The distortion of the spectrum resulting from the attributes of the Si (Li) detector causes a deviation from true values. Silicon internal fluorescence X-rays and incomplete charge collection lead to a concentration overestimation of less than 0.2%. To remove the effect of incomplete charge collection, another correction procedure is needed. Although alkali loss is significant for the analysis of glass, it can be ignored for X-ray collection from areas of more than ~400μm^2. The analytical results using EDS are accurate and comparable to that using the wavelength-dispersive X-ray spectrometer, and we can measure the oxides containing more than 0.7 wt% with a precision of better than 10% RSD.

Table 2. Results of quantitative analysis using the energy-dispersive X-ray spectrometer.

Sample	olivine			clinopyroxene			orthopyroxene			garnet			plagioclase		
Instrument	WDS	EDS (10)	SD.	WDS	EDS (5)	SD.	WDS	EDS (10)	SD.	WDS	EDS (10)	SD.	WDS	EDS (10)	SD.
SiO_2	41.35	41.04	0.23	52.59	53.75	0.36	52.93	53.25	0.34	38.44	37.88	0.13	57.85	58.12	0.33
TiO_2	0.01			0.17	0.19	0.12	0.26	0.27	0.07	0.48	0.48	0.07	0.00		
Al_2O_3	0.00			2.18	2.13	0.17	2.32	2.25	0.06	21.36	20.77	0.06	26.12	26.24	0.23
Cr_2O_3	0.00			0.88	0.86	0.09	0.02			0.00			0.01		
FeO	6.15	6.31	0.16	4.52	4.45	0.30	18.84	18.91	0.24	28.72	28.54	0.24	0.00		
MnO	0.08	0.09	0.07	0.11	0.08	0.05	0.40	0.48	0.13	1.80	1.98	0.07	0.00		
MgO	52.16	52.05	0.21	18.10	18.65	0.27	24.24	24.02	0.12	4.57	4.39	0.06	0.00		
CaO	0.03	0.03	0.02	20.63	21.04	0.08	1.02	1.09	0.07	5.61	5.65	0.07	8.25	8.18	0.12
Na_2O				0.10	0.23	0.05	0.03			0.05			6.99	6.87	0.08
K_2O				0.00			0.00			0.00			0.06	0.18	0.05
NiO	0.40	0.39	0.14	0.00			0.00			0.02			0.00		
Total	100.18	99.91	0.38	99.26	101.38	0.27	100.06	100.26	0.51	101.06	99.70	0.28	99.29	99.58	0.57
Formula															
Si	0.996	0.993		1.932	1.932		1.940	1.947		2.999	3.003		2.607	2.610	
Ti	0.000			0.005	0.005		0.007	0.007		0.028	0.029		0.000		
Al	0.000			0.094	0.090		0.100	0.097		1.964	1.941		1.387	1.389	
Cr	0.000			0.025	0.024		0.000			0.000			0.000		
Fe	0.124	0.128		0.139	0.134		0.577	0.578		1.874	1.892		0.000		
Mn	0.002	0.002		0.003	0.002		0.013	0.015		0.119	0.133		0.000		
Mg	1.873	1.877		0.991	0.999		1.324	1.310		0.532	0.519		0.000		
Ca	0.001	0.001		0.812	0.810		0.040	0.043		0.469	0.480		0.398	0.394	
Na	0.000			0.007	0.016		0.002			0.007			0.611	0.598	
K	0.000			0.000			0.000			0.000			0.004	0.010	
Ni	0.008	0.008		0.000			0.000			0.001			0.000		
Total	3.004	3.007		4.008	4.013		4.004	3.997		7.994	7.997		5.007	5.000	
O	4	4		6	6		6	6		12	12		8	8	

Numbers in parentheses attached to EDS analyses indicate the number of replicated analyses used to calculate the mean and standard deviation (SD.). WDS represents results using the wavelength-dispersive X-ray spectrometer (JEOL JXA-8600) at Niigata University. WDS analysis was performed with a probe current of 1.30 nA and an accelerating voltage of 15 kV, except for olivine (20 nA, 25 kV). The WDS olivine data was provided by Dr. E. Takazawa.

Table 2. (continued)

Sample	K-feldspar			anorthite			glass (NIST 616)				Cr-spinel			ilmenite		
Instrument	WDS	EDS (10)	SD.	WDS	EDS (10)	SD.	R.V.	EDS(6)	SD.		WDS	EDS (5)	SD.	WDS	EDS (4)	SD.
SiO_2	64.91	64.80	0.40	45.14	45.02	0.27	72.00	72.25	0.08	SiO_2	0.09	0.24	0.03	0.1	0.28	0.04
TiO_2	0.05			0.02						TiO_2	0.35	0.28	0.07	49.4	49.85	0.22
Al_2O_3	18.44	18.34	0.17	34.26	34.67	0.10	2.00	2.01	0.03	Al_2O_3	11.50	10.91	0.15	0.0	0.16	0.05
Cr_2O_3	0.00			0.00						Cr_2O_3	51.05	51.31	1.33	0.1	0.06	0.05
FeO	0.03			0.44	0.47	0.09				Fe_2O_3	6.92	5.95	1.21	5.5	4.14	0.41
MnO	0.01			0.00						FeO	22.04	23.34	0.17	43.4	44.41	0.18
MgO	0.00			0.19	0.21	0.05				MnO	0.42	0.51	0.15	0.7	0.54	0.07
CaO	0.00			18.91	18.87	0.18	12.00	11.85	0.04	MgO	7.28	6.49	0.17	0.1	0.03	0.04
Na_2O	0.70	0.58	0.08	0.81	0.88	0.05	14.00	13.90	0.11	CaO	0.04			0.1		
K_2O	15.94	16.09	0.15	0.00						Na_2O	0.04			0.0		
NiO	0.00			0.00						NiO	0.19	0.11	0.09	0.1	0.08	
Total	100.07	99.80	0.63	99.76	100.13	0.32	100	100		Total	99.92	99.14	0.30	99.4	99.55	0.45
Formula										Formula						
Si	2.995	2.999		2.092	2.080					Si	0.003	0.008		0.002	0.007	
Ti	0.002			0.001						Ti	0.009	0.007		0.946	0.951	
Al	1.003	1.000		1.872	1.888					Al	0.455	0.438		0.001	0.005	
Cr	0.000			0.000						Cr	1.355	1.382		0.001	0.001	
Fe	0.001			0.017	0.018					Fe^{3+}	0.175	0.152		0.106	0.079	
Mn	0.000			0.000						Fe^{2+}	0.619	0.665		0.923	0.942	
Mg	0.000			0.013	0.014					Mn	0.012	0.015		0.014	0.012	
Ca	0.000			0.939	0.934					Mg	0.364	0.330		0.002	0.001	
Na	0.062	0.052		0.072	0.079					Ca	0.001			0.002		
K	0.938	0.950		0.000						Na	0.003			0.000		
Ni	0.000			0.000						Ni	0.005	0.003		0.003	0.002	
Total	5.002	5.002		5.007	5.015					O	4	4		3	3	
O	8	8		8	8											

A glass was analyzed with an analytical area of more than 400 μm^2. The composition of glass was normalized to 100%. RV., reference value. Fe_2O_3 and FeO for Cr-spinel and ilmenite were calculated according to Stormer (1983).

Acknowledgements

We wish to thank Associate Prof. E. Takazawa (Niigata Univ.) for the providing a olivine sample and WDS data, together with helpful suggestions; Prof. Y. Hiroi (Chiba Univ), Dr. T. Hokada (NIPR), and Dr. T. Hamamoto (DIA Consultants Co. Ltd.) for their technical advice; and Dr. M.R. Handler (JAMSTEC) for reading and improving the manuscript. This work was supported by Grant-in Aid for Scientific Research (No. 12640441 and 14540420, T. Shimura) from the Japan Society for the Promotion of Science.

References

Devine, J.D., James, E.G., Brack, H.P., Layne, G.D. and Rutherford, M., 1995, Comparison of microanalytical methods for estimating H_2O contents of silicic volcanic glasses. *Am. Mineral.*, **80**, 319-328.

Fujino, M. and Itaya, T., 1992, Quantitative analysis of silicates using energy-dispersive X-ray electronprobe microanalyser -EMAX-2200 at Reserch Center for Microanalysis, Okayama University of Science-. *Bull. Hiruzen Res. Inst., Okayama Univ. Sci.*, **18**, 43-58. (in Japanese)

Gedeon, O., Hulinsky, V. and Jurek, K., 2000, Microanalysis of glass containing alkali ions. *Mikrochim. Acta*, **132**, 505-510.

Goldstein, J., Newbury, D., Joy, D., Lyman, C., Echlin, P., Lifshin, E., Sawyer, L. and Michael, J., 2003, *Scanning Electron Microscopy and X-ray microanalysis*, *third ed.*, Kluwer Academic/Plenum Publ, New York, 689 p.

Kinouchi, S., 2001, *Electron probe microanalyzer*. Gijyutsushoin Publ., Tokyo, 346 p. (in Japanese)

Lineweaver, J.L., 1962, Oxygen outgassing caused by electron bombardment of glass. *J. Appl. Phys.*, **34**, 1786-1791.

Mori, T. and Kanehira, K., 1984, X-ray energy spectrometry for electron-probe analysis. *Jour. Geol. Soc. Japan*, **90**, 271-285.

Nielsen, C.H. and Sigurdsson, H., 1981, Quantitative methods for electron microprobe analysis of sodium in natural and synthetic glasses. *Am. Mineral.*, **66**, 547-552.

Reed, J.B. and Ware, N.G., 1975, Quantitative electron microprobe analsis of silicates using Energy-dispersive X-ray spectrometry. *J. Petrol.*, **16**, 499-519.

Statham, P.J., 1979, A ZAF procedure for microprobe analysis based on measurement of peak to background ratios. *In* Newbur, D.E., ed., *Microbeam analysis*. Sanfrancisco Press, Sanfrancisco, 247-253.

Stormer, J.C., 1983, The effects of recalculation on estimates of temperature and oxygen fugacity from analyses of multi-component iron-titanium oxides. *Am. Mineral.*, **68**, 586-594.

Yokoyama, K., Matsubara, S., Saito, Y., Tiba, T. and Kato, A., 1993, Analyses of natural minerals by energy-dispersive spectrometer. *Bull. Nat. Sci. Mus., Tokyo, Ser. C*, **19**, 115-126.